optica

Surface-enhanced gallium arsenide photonic resonator with quality factor of 6×10^6

Biswarup Guha,[1] Felix Marsault,[2] Fabian Cadiz,[3] Laurence Morgenroth,[4] Vladimir Ulin,[5] Vladimir Berkovitz,[5] Aristide Lemaître,[2] Carmen Gomez,[2] Alberto Amo,[2] Sylvain Combrié,[6] Bruno Gérard,[7] Giuseppe Leo,[1] and Ivan Favero[1,*]

[1]Matériaux et Phénomènes Quantiques, Université Paris Diderot, CNRS UMR 7162, Sorbonne Paris Cité, 10 rue Alice Domon et Léonie Duquet, 75013 Paris, France
[2]Centre de Nanosciences et de Nanotechnologies, CNRS, Université Paris Sud, Université Paris-Saclay, C2N-Marcoussis, Route de Nozay, 91460 Marcoussis, France
[3]Laboratoire de Physique de la Matière Condensée, Ecole Polytechnique, CNRS UMR 7643, Route de Saclay, 91128 Palaiseau, France
[4]Institut d'Electronique, de Microélectronique et de Nanotechnologie, UMR CNRS 8520, Avenue Poincaré, 59652 Villeneuve d'Ascq, France
[5]A. F. Ioffe Physico-Technical Institute, Politekhnicheskaya ul. 26, 194021 Saint Petersburg, Russia
[6]Thales Research and Technology, 1 Avenue Augustin Fresnel, 91767 Palaiseau, France
[7]III-V Lab, 1 Avenue Augustin Fresnel, 91767 Palaiseau, France
*Corresponding author: ivan.favero@univ-paris-diderot.fr

Received 19 September 2016; revised 5 December 2016; accepted 9 January 2017 (Doc. ID 275897); published 9 February 2017

Gallium arsenide and related compound semiconductors lie at the heart of optoelectronics and integrated laser technologies. Shaped at the micro- and nanoscale, they allow strong interaction with quantum dots and quantum wells, and promise stunning optically active devices. However, gallium arsenide optical structures presently exhibit lower performance than their passive counterparts based on silicon, notably in nanophotonics, where the surface plays a chief role. Here, we report on advanced surface control of miniature gallium arsenide optical resonators using two distinct techniques that produce permanent results. One extends the lifetime of free carriers and enhances luminescence, while the other strongly reduces surface absorption and enables ultra-low optical dissipation devices. With such surface control, the quality factor of wavelength-sized optical disk resonators is observed to rise up to 6×10^6 at the telecom wavelength, greatly surpassing previous realizations and opening new prospects for gallium arsenide nanophotonics.

OCIS codes: (140.3945) Microcavities; (230.5750) Resonators; (130.5990) Semiconductors; (240.6670) Surface photochemistry; (130.3120) Integrated optics devices.

https://doi.org/10.1364/OPTICA.4.000218

The ability to strongly confine light is crucial in optical sciences, with applications that span from quantum investigation of light–matter interactions to the advancement of new optical sources, sensors, and detectors. In dielectrics, just like in intrinsic semiconductors, light cannot be steadily localized below half the wavelength in the material [1]. At the telecom wavelength, this leads to ultimate optical mode volumes ranging from few-micrometer cubes down to fraction-of-a-micrometer cubes reached for the most refractive semiconductors. This strong spatial confinement has its temporal counterpart, quantified by the optical quality factor (Q). Over the last decade, Qs in the mid-10^6 and up to 9×10^6 have been progressively obtained with miniature silicon cavities [2,3]. Even though gallium arsenide (GaAs) is just as refractive as silicon, the best GaAs photonic structures have so far saturated an order of magnitude below, with Qs in the mid-10^5 [4–9] and very little progress lately. Reaching the level of silicon nanophotonics with the optically active GaAs material would, however, open many prospects, offering a direct bandgap, strong optical non-linearity, and compliance with versatile emitters like quantum dots and quantum wells. In cavity-QED, the control of single photons and their interactions would improve [10,11]. Nonlinearities at the single-photon level [12,13] would become accessible in GaAs cavities using bulk optical nonlinearity [14–17] or tailored interactions with a mechanical element [18–20]. In polaritonics, the strong coupling regime could be obtained in submicrometer resonators [21]. The performance of miniature GaAs-based lasers [22–28] could also improve, both in threshold and spectral purity. In a recent work, we investigated the case of high-Q (mid-10^5) GaAs whispering gallery resonators and showed that surface absorption was a major source of optical loss [29]. Here we demonstrate advanced surface control and break open the lock associated with surface dissipation. With two distinct techniques—wet nitridation and atomic layer deposition (ALD)—both producing permanent results, we slow down the relaxation of carriers and mitigate the surface absorption currently pinning the performance of devices. As a result, the luminescence of miniature GaAs photonic resonators increases and their optical Q rises up to 6×10^6 at the telecom wavelength, largely surpassing previous demonstrations in GaAs.

Our disk resonators are mounted on an aluminum gallium arsenide (AlGaAs) pedestal [Fig. 1(a)] and are fabricated out

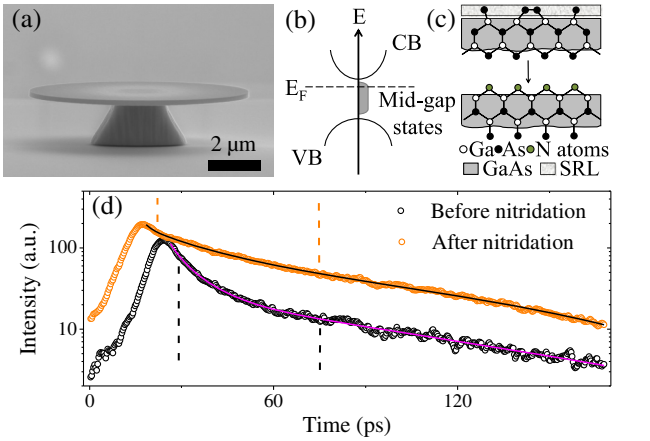

Fig. 1. Wet nitridation of GaAs disk resonators. (a) Electron micrograph of a GaAs disk sitting atop an AlGaAs pedestal. (b) Picture of the intra-gap states formed at the resonator's surface, with arbitrary pinning of the Fermi level E_F set on purpose for illustration. (c) Nitridation process: the surface reconstruction layer (SRL) is replaced by a monolayer of nitrogen atoms. (d) Room-temperature, time-resolved photoluminescence of a GaAs disk before and after nitridation. The decay is fitted by the sum of three exponentials. The intermediate decay, between vertical dashed lines, consistently slows down with nitridation.

of a GaAs(200 nm)/$Al_{0.8}Ga_{0.2}As$(1800 nm)/GaAs epitaxial wafer by electron beam lithography and wet etching [7,29]. Two epitaxial wafers (A and B) of same nominal structure are employed in this work. With a radius of a few micrometers, the disks support whispering gallery modes (WGMs) in the telecom range with bending loss Q higher than 10^8. In practice, our best resonators have to date reached $Q = 5 \times 10^5$, and we have established that the reconstruction layer at the resonator's surface was playing a central part in this discrepancy [29]. Indeed the associated electronic states within the gap of the material, represented in Fig. 1(b), imply possible absorption of photons below the bandgap. By controlling the structural and chemical nature of the surface, the density of mid-gap states and the Fermi level pinning can be tuned, producing variable effects on optical absorption, carrier dynamics, and luminescence.

We first investigate a process of wet nitridation based on a hydrazine (N_2H_4) solution, leading to the formation of a stable GaN layer on the surface [Fig. 1(c)]. Surface nitridation has been shown to enhance the photoluminescence of bulk GaAs under continuous-wave pumping [30], but it is accompanied by detrimental surface etching. In order to preserve our miniature resonators, we intentionally lower the pH of the solution and bring parasitic etching to a negligible amount. We observe a marked effect of the resulting surface treatment in room-temperature, time-resolved photoluminescence experiments performed on individual disk resonators. A time trace of photoluminescence is reported in Fig. 1(d) and reveals a rich dynamic, with a decay fitted by the sum of a rapid (τ_1), intermediate (τ_2), and slow (τ_3) exponential function [31,32]. The intermediate decay time τ_2 corresponds to the relaxation of carriers responsible for luminescence. This decay is systematically slowed down by surface nitridation, with τ_2 increasing from 7.7 ± 1 to 18 ± 3 ps, while the other decay times are essentially unaffected (see Supplement 1). Under continuous pumping, the steady-state luminescence of a single disk experiences a 20-fold enhancement, with no visible degradation over a month. However, these pronounced effects on the carrier dynamics and luminescence do not show counterparts in terms of optical absorption. Our measurement of GaAs disk WGMs with a fiber taper [33] show neither improvement of Qs nor reduction of absorption after nitridation. The situation changes, however, when other passivation methods are instead employed.

A second surface control technique consists of Atomic Layer Deposition (ALD) of alumina (Al_2O_3), which produces extremely thin, uniform, and conformal layers on the surface (see Supplement 1). Figure 2 shows the optical spectrum of a single GaAs disk resonator before and after ALD treatment. The spectra reveal a series of fine WGM resonance dips [7,33], spreading over 100 nm in wavelength. These resonances bunch in distinct groups, separated by the free spectral range associated with adjacent WGM azimuthal numbers [34]. After ALD, the structure of the spectrum is preserved but a global shift is observed (see Supplement 1). The optical resonances are narrowed while their contrast increases, pointing toward reduction of losses. A finer understanding is provided by experiments at higher optical power.

Figure 3 shows selected WGM resonances of a GaAs disk resonator, measured before and after ALD. At low power, the WGM resonance in Figs. 3(a) and 3(b) adopts a Lorentzian shape and is narrowed by a factor 2.3 after ALD, with a constant contrast of 40%. In the coupled-mode theory (CMT) of fiber/disk coupling experiments [7,33], this implies a 2.3-fold reduction of the intrinsic loss rate of the WGM κ_{in}. At high power, the resonance is distorted by thermo-optical effects, with a wavelength drag corresponding to the rise of disk temperature produced by absorption [29]. In Figs. 3(c) and 3(d), a second WGM resonance experiences an important reduction of this drag after ALD treatment, which, in

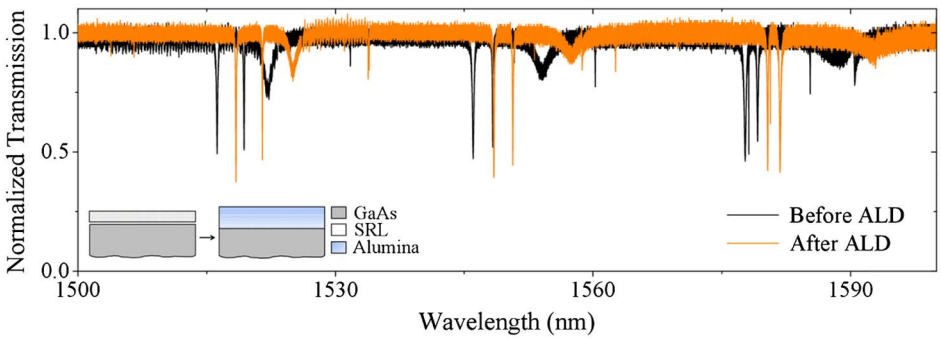

Fig. 2. Effect of ALD surface treatment on the optical spectrum of a GaAs disk resonator. After removal of the surface reconstruction layer (SRL) and 20 nm alumina deposition in this example, WGM resonances are redshifted and narrowed, and new thin resonances appear with low contrast. The disk thickness (radius) is 200 nm (4.5 μm). All WGMs are TE polarized and identified in Supplement 1.

Supplement 1, is shown to correspond to an absorption reduction by a factor of 7.7. On top of this pronounced absorption reduction, ALD can also positively impact scattering losses [35,36] of WGMs of moderate Q (see Supplement 1). In our most-performing GaAs disks, with ultra-smooth surfaces, the optical Q of the best WGMs was mainly limited by surface absorption [29] with a second-order role of scattering losses; hence, ALD passivation must produce pronounced results in this case.

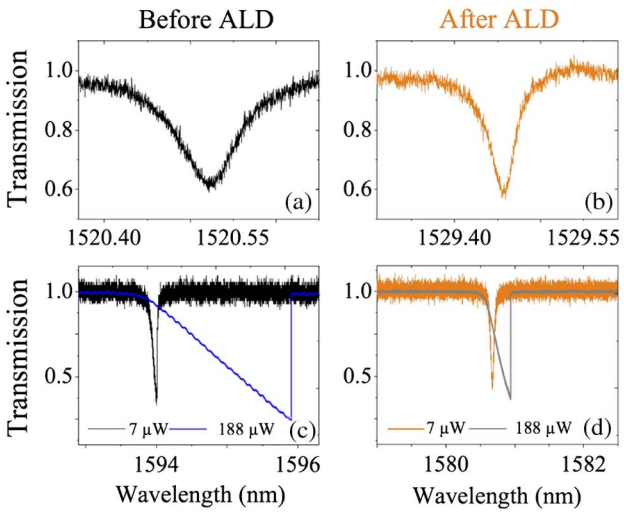

Fig. 3. Reduction of optical absorption by ALD passivation. (a) Selected WGM resonance (TE $p = 5$) of a 4.5 μm radius GaAs disk, measured at low optical power before ALD, with FWHM of 84 pm. (b) Same resonance after ALD, with FWHM of 36 pm. The deposition is of 20 nm of alumina, which redshifted the resonance. This disk did not experience ammonia dip prior to ALD. (c, d) show another WGM resonance (TE $p = 3$) on another disk of radius 3.4 μm, showing thermo-optical shift of (c) 1.914 nm before and (d) 261 pm after ALD with 30 nm of alumina. The blueshift is attributed to a combination of hydrogen plasma and ammonia dip prior to ALD (see Supplement 1).

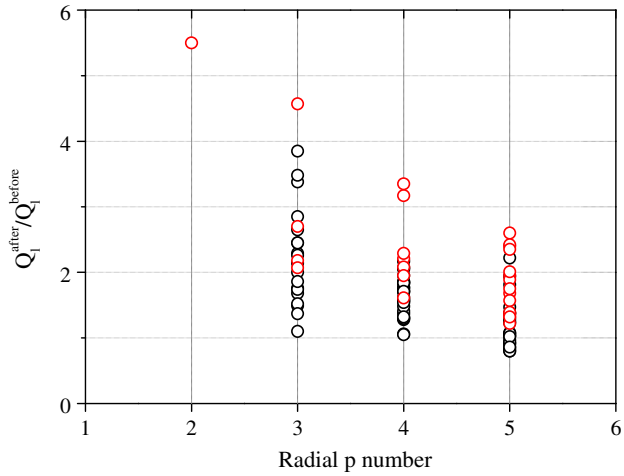

Fig. 4. Modal dependence of the Q enhancement obtained by ALD. The enhancement of the loaded Q_l is measured at constant contrast of the optical resonance as a function of the WGM radial number p and for two distinct wafers A (black) and B (red). All measured disks have same radius (thickness) of 4.5 μm (200 nm). All modes are TE, and typically show Qs in the 10^4 to 10^5 range (under-coupled). The ALD layer thickness is between 5 and 30 nm (see Supplement 1).

We investigate how the ALD influence on Q is impacted by the WGM mode profile and the quality of the employed wafer. In Fig. 4 we show the measured Q enhancement obtained by ALD for WGMs of different radial order p [34] and for the two epitaxial wafers A and B. Qs are analyzed in a loaded configuration producing constant resonance contrast of 50%. In such configuration, the measured enhancement factor varies between 1 and 6 for p between 2 and 5. A first observation is that the Q enhancement improves as p decreases, corresponding to a localization of electromagnetic energy at the surface. This further supports the idea that the main source of optical dissipation in high-Q GaAs WGMs lies at surfaces [29]. WGMs of $p = 1$ were not experimentally accessible before ALD in this data series, such that their improvement factor (expected above 6) is not available in Fig. 4. The second observation is the qualitatively different behavior of wafers A and B. Both wafers are expected to possess a residual p-doping below $10^{15}/\text{cm}^3$ range; however, the Q enhancement is more pronounced for wafer B, pointing toward less residual bulk absorption. This illustrates that with Qs approaching the 10^6 range, previously insignificant variations of the crystal quality may now matter. In Supplement 1, we show that improvement factors do not vary when the deposited alumina thickness increases from 5 to 10, 20, and 30 nm. This indicates that a layer of 5 nm suffices to obtain the beneficial features reported in this work.

Figure 5 reports systematic fiber-taper optical measurements performed at low power on an ALD-passivated GaAs disk of radius 4.5 μm. The upper panel of Fig. 5 is a TE WGM ($p = 1$) spectrum obtained in the under-coupled regime, which

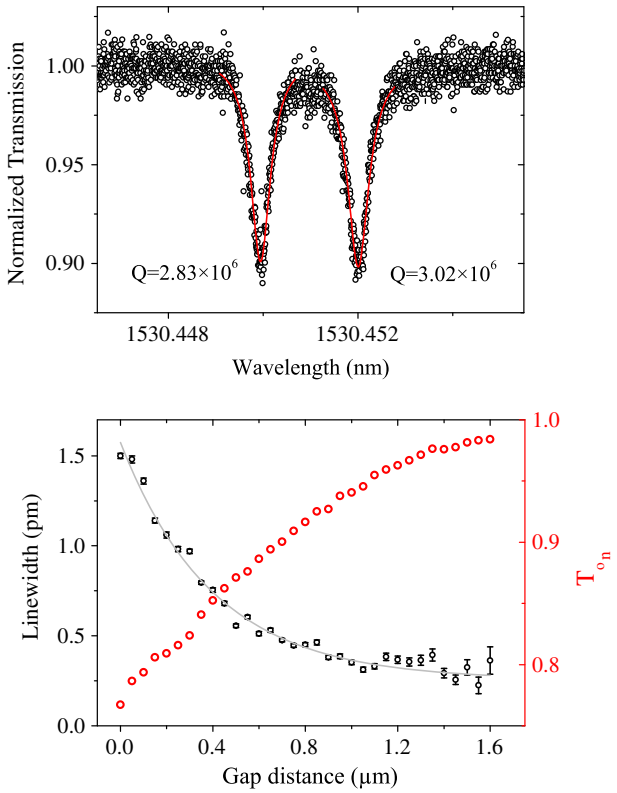

Fig. 5. GaAs disk WGM with a Q of 6×10^6. (a) Under-coupled optical spectrum of an ultra-high Q TE WGM ($p = 1$) measured on a disk of radius (thickness) 4.5 μm (200 nm) treated by ALD. (b) Line width and resonant transmission of the WGM resonance as function of the fiber–resonator gap distance, showing intrinsic Q of 6×10^6.

reveals a fine-structure doublet typical of a high-Q situation [7,33]. The loaded Q for each component of the doublet is 2.8×10^6 and 3×10^6, an order of magnitude above results obtained on same disks without surface treatment [33]. In order to disentangle dissipative effects associated with the presence of the fiber taper, we vary the gap distance between the taper and resonator (see lower panel of Fig. 5). At large gap distance, the line width of the resonance converges to an intrinsic value of 0.26 ± 0.03 pm, corresponding to an intrinsic Q of $5.9(\pm 0.6) \times 10^6$. We observe similar values on several WGMs and resonators having experienced the same surface treatment. Typically 25% of our resonators, once ALD treated, show WGMs rising up over 10^6 in Q. The results shown here represent a 10-fold improvement with respect to prior state of the art in GaAs photonic cavities, and clearly underline the potential of proper surface control. Interestingly, these ultra-high-Q WGMs coupled to a fiber taper do not behave as expected from standard CMT [37], in contrast to the case of smaller Qs [7,33]. At 500 nm gap distance, Fig. 5 shows that the fiber taper presence increases the WGM line width by a factor of 2, while the contrast hardly reaches 20% instead of the 100% expected from CMT in this case.

In conclusion, novel surface control techniques enable bringing GaAs photonic cavities to a new stage. Even though we have not yet reached the theoretical limit set by bending losses, the presented WGM resonators already attain optical Qs in the 10^6 range and up to 6×10^6. The results reported here show no degradation upon time, with a stability observed over a month under ambient laboratory conditions. These advances should be beneficial to multiple fields of research utilizing GaAs photonics such as solid-state cavity QED, nonlinear optics, optoelectronics, and optomechanics [6,7]. Interestingly, the two surface treatments employed here somehow provide contradictory trends: one (nitridation) slows down carrier relaxation but does not impact optical surface absorption at 1.55 μm, while the other (alumina ALD) strongly reduces surface absorption but produces variable effects on carrier relaxation [38]. These observations call for a better understanding of the exact relation between microscopic aspects such as spectral density of surface states, surface pinning of the Fermi level, or surface chemical state, and measured properties like the optical and transport responses of the resonator at various frequencies. In the context of optomechanics, for metrological and quantum applications, the impact of these microscopic aspects on mechanical dissipation [39,40] will also be of utmost importance. Nanoscale GaAs resonators, just like those made out of other materials including silicon [3,41,42], will require advanced surface physics and engineering to reveal their scientific potential in full.

Funding. Agence Nationale de la Recherche (ANR)–Direction Générale de l'Armement (DGA) (Octopuss); European Research Council (ERC) (306664).

Acknowledgment. We thank Daniel Paget and David Parrain for their first attempts toward the surface control of GaAs disks.

See Supplement 1 for supporting content.

REFERENCES

1. J. B. Khurgin, Nat. Nanotechnol. **10**, 2 (2015).
2. Y. Taguchi, Y. Takahashi, Y. Sato, T. Asano, and S. Noda, Opt. Express **19**, 11916 (2011).
3. H. Sekoguchi, Y. Takahashi, T. Asano, and S. Noda, Opt. Express **22**, 916 (2014).
4. C. P. Michael, K. Srinivasan, T. J. Johnson, O. Painter, K. H. Lee, K. Hennessy, H. Kim, and E. Hu, Appl. Phys. Lett. **90**, 051108 (2007).
5. S. Combrie, A. De Rossi, Q. V. Tran, and H. Benisty, Opt. Lett. **33**, 1908 (2008).
6. L. Ding, C. Baker, P. Senellart, A. Lemaître, S. Ducci, G. Leo, and I. Favero, Phys. Rev. Lett. **105**, 263903 (2010).
7. J. C. L. Ding, C. Baker, A. Andronico, D. Parrain, P. Senellart, A. Lemaître, S. Ducci, G. Leo, and I. Favero, *Handbook of Optical Microcavities* (PanStanford, 2014).
8. C. Arnold, V. Loo, A. Lemaître, I. Sagnes, O. Krebs, P. Voisin, P. Senellart, and L. Lanco, Appl. Phys. Lett. **100**, 111111 (2012).
9. S. Reitzenstein, C. Hofmann, A. Gorbunov, M. Strauss, S. H. Kwon, C. Schneider, A. Löffler, S. Höfling, M. Kamp, and A. Forchel, App. Phys. Lett. **90**, 251109 (2007).
10. E. Peter, P. Senellart, D. Martrou, A. Lemaître, J. Hours, J. M. Gérard, and J. Bloch, Phys. Rev. Lett. **95**, 067401 (2005).
11. K. Srinivasan and O. Painter, Nature **450**, 862 (2007).
12. A. Faraon, I. Fushman, D. Englund, N. Stoltz, P. Petroff, and J. Vuckovic, Nat. Phys. **4**, 859 (2008).
13. V. Loo, C. Arnold, O. Gazzano, A. Lemaître, I. Sagnes, O. Krebs, P. Voisin, P. Senellart, and L. Lanco, Phys. Rev. Lett. **109**, 166806 (2012).
14. M. Bamba, A. Imamoğlu, I. Carusotto, and C. Ciuti, Phys. Rev. A **83**, 021802(R) (2011).
15. A. Andronico, I. Favero, and G. Leo, Opt. Lett. **33**, 2026 (2008).
16. P. S. Kuo, J. Bravo-Abad, and G. S. Solomon, Nat. Commun. **5**, 3109 (2013).
17. S. Mariani, A. Andronico, A. Lemaître, I. Favero, S. Ducci, and G. Leo, Opt. Lett. **39**, 3062 (2014).
18. A. Nunnenkamp, K. Børkje, and S. M. Girvin, Phys. Rev. Lett. **107**, 063602 (2011).
19. P. Rabl, Phys. Rev. Lett. **107**, 063601 (2011).
20. J. Restrepo, C. Ciuti, and I. Favero, Phys. Rev. Lett. **112**, 013601 (2014).
21. D. Bajoni, P. Senellart, E. Wertz, I. Sagnes, A. Miard, A. Lemaître, and J. Bloch, Phys. Rev. Lett. **100**, 47401 (2008).
22. U. Mohideen, W. S. Hobson, S. J. Pearton, F. Ren, and R. E. Slusher, Appl. Phys. Lett. **64**, 1911 (1994).
23. K. Srinivasan, M. Borselli, T. J. Johnson, P. E. Barclay, O. Painter, A. Stintz, and S. Krishna, Appl. Phys. Lett. **86**, 151106 (2005).
24. F. Albert, T. Braun, T. Heidel, C. Schneider, S. Reitzenstein, S. Höfling, L. Worschech, and A. Forchel, Appl. Phys. Lett. **97**, 101108 (2010).
25. A. Tandaechanurat, S. Ishida, D. Guimard, M. Nomura, S. Iwamoto, and Y. Arakawa, Nat. Photonics **5**, 91 (2010).
26. B. Ellis, M. A. Mayer, G. Shambat, T. Sarmiento, J. Harris, E. E. Haller, and J. Vučković, Nat. Photonics **5**, 297 (2011).
27. D. Saxena, S. Mokkapati, P. Parkinson, N. Jiang, Q. Gao, H. Hoe Tan, and C. Jagadish, Nat. Photonics **7**, 963 (2013).
28. J. Tatebayashi, S. Kako, J. Ho, Y. Ota, S. Iwamoto, and Y. Arakawa, Nat. Photonics **9**, 501 (2015).
29. D. Parrain, C. Baker, G. Wang, B. Guha, E. Gil-Santos, A. Lemaître, P. Senellart, G. Leo, S. Ducci, and I. Favero, Opt. Express **23**, 19656 (2015).
30. V. L. Berkovits, D. Paget, A. N. Karpenko, V. P. Ulin, and O. E. Tereshchenko, Appl. Phys. Lett. **90**, 022104 (2007).
31. R. Eccleston, R. Strobel, W. W. Rühle, J. Kuhl, B. F. Feuerbacher, and K. Ploog, Phys. Rev. B **44**, 1395 (1991).
32. A. Amo, M. D. Martín, L. Viña, A. I. Toropov, and K. S. Zhuravlev, Phys. Rev. B **73**, 035205 (2006).
33. L. Ding, P. Senellart, A. Lemaître, S. Ducci, G. Leo, and I. Favero, Proc. SPIE **7712**, 771211 (2010).
34. A. Andronico, X. Caillet, I. Favero, S. Ducci, V. Berger, and G. Leo, J. Eur. Opt. Soc. **3**, 08030 (2008).
35. T. Alasaarela, D. Korn, L. Alloatti, A. Saynatjoki, A. Tervonen, R. Palmer, J. Leuthold, W. Freude, and S. Honkanen, Opt. Express **19**, 11529 (2011).
36. A. Khanna, A. Z. Subramanian, M. Häyrinen, S. Selvaraja, P. Verheyen, D. Van Thourhout, S. Honkanen, H. Lipsanen, and R. Baets, Opt. Express **22**, 5684 (2014).
37. S. M. Spillane, T. J. Kippenberg, O. J. Painter, and K. J. Vahala, Phys. Rev. Lett. **91**, 043902 (2003).
38. G. Moille, S. Combrié, L. Morgenroth, G. Lehoucq, F. Neuilly, B. Hu, D. Decoster, and A. de Rossi, Laser Photon. Rev. **10**, 409 (2016).
39. D. T. Nguyen, C. Baker, W. Hease, S. Sejil, P. Senellart, A. Lemaître, S. Ducci, G. Leo, and I. Favero, Appl. Phys. Lett. **103**, 241112 (2013).
40. D. T. Nguyen, W. Hease, C. Baker, E. Gil-Santos, P. Senellart, A. Lemaître, S. Ducci, G. Leo, and I. Favero, New J. Phys. **17**, 023016 (2015).
41. M. Borselli, T. J. Johnson, and O. Painter, Appl. Phys. Lett. **88**, 131114 (2006).
42. M. Borselli, T. J. Johnson, C. P. Michael, M. D. Henry, and O. Painter, Appl. Phys. Lett. **91**, 131117 (2007).